Nonlinear and scaling properties of the dielectric response of $SrTi^{18}O_3$ in the quantum paraelectric regime

Jan Dec,[1,2,*] Wolfgang Kleemann,[1] and Mitsuru Itoh[3]
[1]*Angewandte Physik, Universität Duisburg-Essen, D-47048 Duisburg, Germany*
[2]*Institute of Physics, University of Silesia, Pl-40-007 Katowice, Poland*
[3]*Materials and Structures Laboratory, Tokyo Institute of Technology, Midori, Yokohama 226-8503, Japan*
(Received 10 December 2004; published 28 April 2005)

Critical behavior, scaling, and nonlinear properties of the susceptibility $\chi^* = \chi' - i\chi''$ in ^{18}O isotope exchanged $SrTiO_3$ are revisited in a crystal that was perfectly single domained by an external electric field in the quantum paraelectric regime above $T_c \approx 24$ K. Corrections due to random-field induced nanoregions turn out to be important, if not decisive, for a reliable description. We find quantum critical exponents $\gamma = 1.9 \pm 0.1$, $\delta = 2.7 \pm 0.1$, and $\Delta = 3.1 \pm 0.1$, and a divergency of the nonlinearity coefficient B with an exponent $3\gamma - 2\Delta \approx -0.4$. Below T_c critical and scaling analysis is inhibited by large contributions of domain walls to the susceptibility.

DOI: 10.1103/PhysRevB.71.144113 PACS number(s): 77.80.Bh, 77.80.Fm, 77.84.Dy, 77.22.−d

I. INTRODUCTION

Strontium titanate $SrTiO_3$ (STO) takes a very particular position among the oxygen-octahedral compounds with perovskite-type structure. Many findings, new original concepts and ideas in the physics of phase transitions or even more generally in condensed matter physics, have been born and developed when investigating this unique material.[1] On one hand, STO reveals one of the rare antiferrodistorsive structural phase transition from cubic $Pm3m$ to tetragonal $I4/mcm$ symmetry at $T_a \simeq 105$ K with criticality of the order parameter as first explored by Müller *et al.*[2] Ever since it has been regarded as a model system for displacive phase transitions. Further, the appearance of quantum paraelectricity in pure STO (Ref. 3) and ferroelectricity in STO doped with Ca^{2+} ions[4] or chemically equivalent, but heavier oxygen ions $^{18}O^{2-}$ (STO18),[5] has attracted unrivalled interest in the low temperature properties of this compound.

The nature of the ferroelectric phase transition induced by the exchange of oxygen ^{16}O by its isotope ^{18}O and of the low temperature ferroelectric state thus obtained still remains controversial. This is manifested both in theoretical and experimental research. While Bussmann-Holder *et al.*[6] and Kvyatkovskii[7] predict a displacive soft-mode mechanism of the phase transition into a conventional ferroelectric state in their theoretical works, Yamada *et al.*[8] claim that STO18 undergoes a transition into a three state quantum order-disorder system. Its very specific "ferroelectric" phase is expected to reveal a considerable amount of polarization fluctuations even at $T = 0$ K, associated with tunneling fluctuations of the dipoles. Actually, the order-disorder nature of this phase transition was originally suggested by Zhang *et al.*[9] Its microscopic symmetry is still under debate. While common belief would favor an orthorhombic symmetry with the spontaneous polarization and the easy axis of susceptibility lying in the c plane as in STO:Ca,[4] optical second harmonic generation (SHG)[10] and very recent NMR studies[11] favor a lower symmetry, probably a triclinic space group. In this paper we focus on the paraelectric regime, where the easy axis of susceptibility lies along $[110]_c$.

Similarly, in experimental research, one kind of experiments clearly indicates a structural phase transition at $T_c \approx 24$ K into a mesoscopic domain state[10,12–15] or even into a normal ferroelectric[16] state with lowered symmetry, while others, e.g., x-ray or neutron diffraction and heat capacity, could not detect any anomalies near T_c,[5,17] thus indicating that the system rather transforms into a disordered or very short-ranged polar state.

Having in mind the above ambiguities we decided to carry out detailed investigations of the nonlinear dielectric response of the STO18 system, since it is believed that the nonlinear susceptibility is more sensitive to dipolar ordering than the linear one.[18] These investigations are to shed some light on the nature of the phase transition and the low-temperature phase of STO18. In the present experiments special attention is paid to investigations on samples in the tetragonal single domain state when cooling to below T_a. This state of the sample is an essential prerequisite for reliable experimental data. Very probably, some of the contradictions found in the experimental results hitherto reported may originate from ill-defined multidomain states of the samples investigated. Here we name our own previous work[19] and that of others,[20] which differs in some important details. Although most authors used the shaping method[21] for obtaining a single domain state in the samples, it has been demonstrated that these conditions are insufficient for obtaining the single domain state in the STO18 single-crystal sample.[15,22,23] Surprisingly, this deficiency can be remedied by additionally applying a dc electric field which efficiently supports this procedure.[24]

II. EXPERIMENTAL PROCEDURE

The experiments were performed on a single crystal sample of $SrTi(^{16}O_{0.06}, ^{18}O_{0.94})_3$ prepared in the same way as described previously[5,25] with dimensions $10 \times 2 \times 0.5$ mm^3 along the directions $[1\,0\,0]_c$, $[\bar{1}\,1\,0]_c$, $[1\,1\,0]_c$ (in the cubic

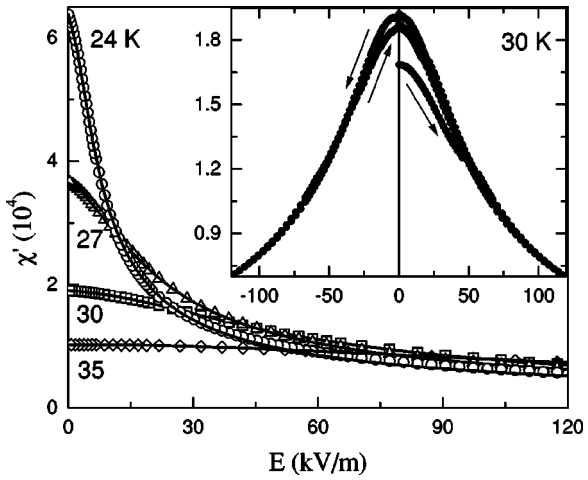

FIG. 1. dc electric-field dependences of the electric susceptibility at selected temperatures $T=24$, 27, 30, and 35 K and their best fits (solid lines) as measured in the sixth quarters of continuous hysteresis cycles. The inset shows one complete experimental cycle masured at 30 K. For clarity only every second experimental point is shown.

system), respectively. Following Bednorz and Müller,[4] the sample was etched in boiling orthophosphoric acid in order to remove surface layers of about 0.1 mm thickness. After this procedure the sample reached its final size $10\times1.9\times0.3$ mm^3, and according to common expectation[21] this geometry should warrant formation of a crystallographic single domain state with the tetragonal c axis along the long sample edges when cooling to below T_a. Vacuum deposition of a thin copper interface and subsequent rf sputtering of gold were used to cover the major $(110)_c$ faces with electrodes. The linear susceptibility $\chi^*=\chi'-i\chi''$ was measured using a Hewlett-Packard 4192-A impedance analyzer at the frequency $f=10$ kHz, temperatures $4<T<50$ K and an amplitude of the ac probing field $E=30$ V/m in a helium-gas-flow cryostat. Starting from $E=0$, the bias field was swept between ±120 kV/m at constant temperature. In order to warrant identical conditions for all measurements, prior to each measurement carried out, the sample was refreshed at $T=150$ K for half an hour and then cooled down in zero field to the required temperature.

III. EXPERIMENTAL RESULTS AND DISCUSSION

A. Electric field control of structurally single domained sample

Figure 1 shows representative examples of the dependence of electric susceptibility on the dc bias field as observed in the sixth quarters of the respective complete loops measured at $T\geqslant T_c\simeq24$ K.[5,16] An example of such a bell-shaped complete loop taken at 30 K is shown in the inset. Solid lines represent fits to a model described below. The bias field was applied step by step when cycling between $\pm E_{\max}$ in order to record 1.5 periods, i.e., six quarters, of the loop at fixed temperatures. At this temperature, being far above the ferroelectric phase transition temperature, the sample still remains in the paraelectric state. It is seen from the inset in Fig. 1 that the curve related to the first quarter differs substantially from the others. This primary curve starts markedly below the apex of the bell, and the susceptibility decreases monotonically when increasing the bias field up to about 50 kV/m. At this field a jerky increase of the susceptibility takes place, which is spread over a field interval of about $\Delta E\approx10$ kV/m. After reaching a new equilibrium state the monotonic decrease of the response continues until the maximum bias field is attained. On subsequent decreasing of the bias field, the susceptibility monotonically increases again, following the primary run in the high field limit. However, below $E\approx70$ kV/m it deviates from the primary curve reaching values enlarged by about 15% (inset in Fig. 1). On further cycling only very minute further changes are observed (solid and open triangles in Fig. 1). This reflects near-reproducibility of the susceptibility data after the sixth quarter cycle. It is these data that are subject to detailed analysis in the present paper. The initial discontinuous recovery of the χ vs E curve is attributed to an electric field induced switching of ferroelastic domains.[24] Obviously, the shaping conditions alone[21] are insufficient to form a single domain state in STO18 and a dc electric field may be used to switch the residual domains as discussed in detail elsewhere.[24]

B. Electric field dependent linear susceptibility

As shown in Fig. 1 an extremely strong field dependence of the dielectric susceptibility is observed when approaching T_c from above. While χ' is nearly independent of E for $T\geqslant35$ K, a drastic drop of the susceptibility is observed on the isotherm related to $T_c=24$ K, where it is reduced by a factor of approximately 6.5 from its initial value when approaching $E_{\max}=120$ kV/m. Characteristically, the main part of this reduction happens in the low field limit $E\leqslant20$ kV/m. Another issue that comes from Fig. 1 is that the strong nonlinearity of the dielectric response in the paraelectric phase is restricted to a relatively narrow temperature range between T_c and T_c+10 K.

In order to describe the experimental data phenomenologically we decided to start from the well-known two-termed electric equation of state

$$E = AP + BP^3, \tag{1}$$

where P is the polarization induced be the applied electric field E and $A=A_0(T-T_c)$ is a temperature-dependent coefficient. A_0 is a constant and B the so-called nonlinearity coefficient which is assumed to be temperature-independent in classic Landau approximation. Equation (1) is expected to be valid for small enough values of the polarization where higher terms of P in Eq. (1) can be neglected. Equation (1) provides the relationship between the electric field and the induced polarization, from which the relationship between the electric susceptibility and the electric field may easily be deduced as

$$\partial E/\partial P = 1/(\varepsilon_0\chi') = A + 3BP^3, \tag{2}$$

where ε_0 is the permittivity of the free space. For practical use an explicit function for $\chi'(E)$ is preferred,

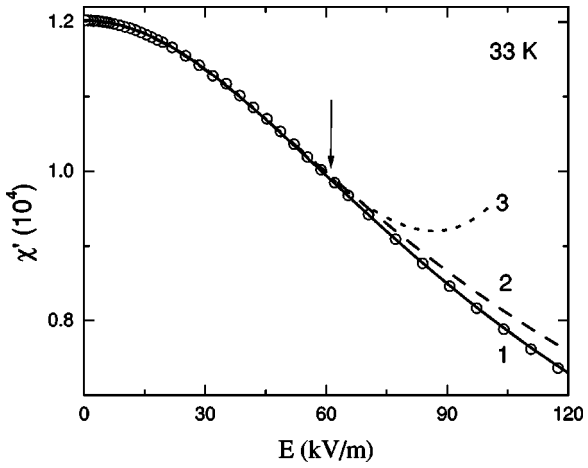

FIG. 2. dc electric-field dependence of the electric susceptibility taken at 33 K and their best fits to Eqs. (3) and (4) (solid line 1), Eq. (5) (dashed line 2), and Eq. (6) (dotted line 3), respectively. The vertical arrow designates the fitting range for lines 2 and 3. For clarity only every second experimental point is shown.

$$\chi'(E) = 1/(\varepsilon_0 A + 3\varepsilon_0 B P^2), \tag{3}$$

where the explicit relationship for $P(E)$ has to be incorporated into Eq. (3). This may be obtained analytically from Eq. (1) as a solution of the tertiary equation

$$P(E) = [-q/2 + (D)^{1/2}]^{1/3} - [q/2 + (D)^{1/2}]^{1/3}, \tag{4}$$

with a new variable $q=-E/B$ and a positive discriminant $D=(p/3)^3+(q/2)^2>0$, where $p=A/B$. Equations (3) and (4) provide a convenient expression for $\chi'(E)$, which contains only two adjustable fitting parameters A and B. What is even more important, it is based on the identical approximation as the initial equation of state Eq. (1), which is in fact the inverse function of Eq. (4). In Fig. 2 the sixth quarter data taken at 33 K are shown. The solid line (line 1) represents a best fit of these data to Eqs. (3) and (4). The fitting procedure was carried out in the whole data range and the result has appeared to be very satisfactory as indicated by a very low value of the chi-square function $\chi^2=125.9$, a favorable value of the correlation coefficient $R^2=0.99994$ and very precisely determined values of the fitting parameters $A=(9.3959\pm0.0013)\times10^6$ V m/C and $B=(1.837\pm0.002)\times10^{10}$ m^5 V/C^3, respectively.

It is interesting to compare this result with other approximate treatments, which have been developed in order to obtain $\chi'(E)$. One of them was proposed by Johnson,[26]

$$\chi'(E) = \chi_1/[1 + 3B(\varepsilon_0\chi_1)^3 E^2]^{1/3}, \tag{5}$$

which also contains two fitting parameters, the initial linear susceptibility χ_1 and B. In order to obtain the same low value of χ^2 as in the previous treatment the fitting range has to be reduced by one half, i.e., by fitting only the data below $E\approx60$ kV/m as indicated by the vertical arrow in Fig. 2. In this case the values $\chi_1=12021\pm2$ and $B=(5.713\pm0.014)\times10^{10}$ m^5 V/C^3 with $\chi^2=120.1$ and $R^2=0.99969$, respectively, are obtained. It is seen that the value of B is now more than three times larger and its standard deviation is one order of magnitude larger. An extrapolation of the best-fitting broken line (line 2) in Fig. 2 beyond the fitting range deviates appreciably from the experimental data. Otherwise, when fitting Eq. (5) to the data in the whole range of data presented in Fig. 2 much larger values of χ^2 and R^2 are obtained. The most popular expression for $\chi'(E)$ has the form of a series of even-power terms in the electric field E,[27,28]

$$\chi'(E) = \chi_1 - 3\chi_3 E^2 + 5\chi_5 E^4 \mp \cdots, \tag{6}$$

where the expansion parameters $\chi_1=1/(\varepsilon_0 A)$, $\chi_3=B/(\varepsilon_0 A^4)$, $\chi_5=3B^2/(\varepsilon_0 A^7)$, etc., are related to the equation of state Eq. (1). The above series contains an infinite number of terms with an infinite number of χ parameters, all of which may be expressed by the coefficients A and B appearing in Eq. (1). When expanding the equation of state, as well, into an infinite power series, the χ parameters have to be redefined, respectively. Approximate features of Eq. (6) containing the first three terms are illustrated in Fig. 2 by the dotted line (line 3). Its extrapolation beyond the fitting range (vertical arrow) deviates significantly from the data. While the χ-square and R^2 functions were, again, similar as in the previous cases, $\chi^2=123.0$ and $R^2=0.99972$, respectively, the fitting expression now contains three adjustable parameters $\chi_1=12012\pm2$, $\chi_3=(2.493\pm0.015)\times10^{-7}$ m^2/V^2, and $\chi_5=(9.9\pm0.3)\times10^{-18}$ m^4/V^4, which yield $A=(9.3955\pm0.0016)\times10^6$ V m/C and $B=(1.720\pm0.013)\times10^{10}$ m^5 V/C^3 in good agreement with the results of the first fit. The value of B is slightly smaller, which is probably due to a different number of experimental points analyzed in both procedures. While in the first procedure the entire curvature of the data is taken into the account, data beyond the inflection point are omitted when using Eq. (6). Hence, very probably the fit based on Eqs. (3) and (4) and its value of B seem to be more adequate for the system investigated.

The above discussion shows that the very simple equation of state (1) offers a very powerful tool for an effective evaluation of realistic data in a relatively large range of electric fields. Obviously the expression (4) may be expanded into a series

$$P(E) = E/A - BE^3/A^4 + 3B^2E^5/A^7 \mp \cdots \tag{7}$$

under the constraint that $27BE^2/(4A^3)<1$. After differentiation, $\partial P/\partial E=\varepsilon_0\chi'(E)$, one obtains an expression for $\chi'(E)$ which is identical with the series in Eq. (6). It is obvious that the series expansions in Eq. (6) or (7), cut off after the third term, are less powerful in fitting the data than the combination of Eqs. (3) and (4), which make use of all information contained in the equation of state. Thus the series expression (6) may only be used in cases, where a very weak field dependence of susceptibility is involved. As seen in Fig. 1, this is not the case for STO18. In the case of strong nonlinearity rather the rigorous expressions based on the equation of state Eq. (1), Eqs. (3) and (4), have to be used.

The above fitting procedure is satisfactory for the isotherms recorded in the temperature range of $31\leqslant T\leqslant50$ K. However, at $T=30$ K a significant increase of the chi-square function $\chi^2=3784$, and a reduction of the correlation coefficient $R^2=0.99977$ emerges from a best fit according to Eqs.

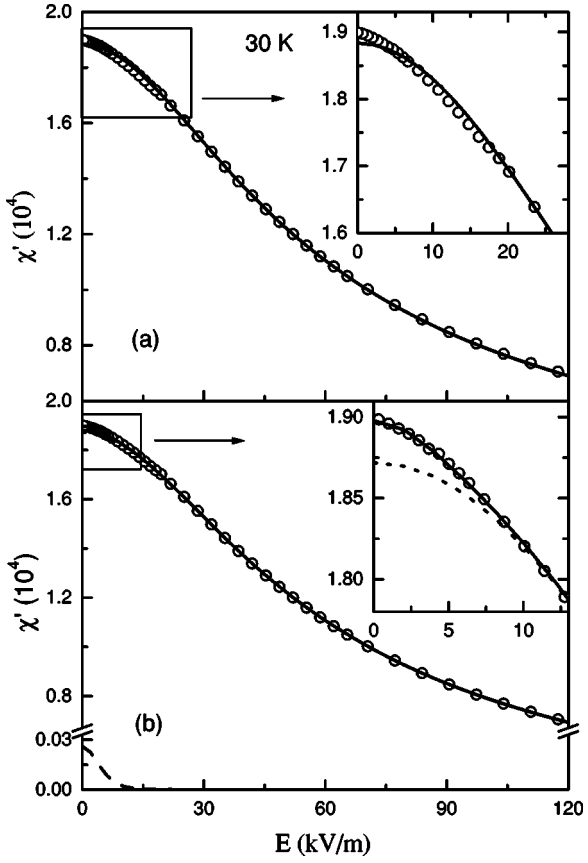

FIG. 3. dc electric-field dependence of the electric susceptibility taken at 30 K and their best fits according to the one component (3a) and the two component (3b) polarization mechanism, respectively. The insets show details in the low field limit. For clarity only every second experimental point is shown.

(3) and (4) [Fig. 3(a)]. In particular, severe deviations of the fitting curve from experimental data are observed in the low field limit [Fig. 3(a), inset]. This behavior indicates that the relatively poor fit cannot be due to the truncation of the equation of state consisting of two terms only. Higher-order terms in Eq. (1) would rather improve the situation in the high field range. The above symptoms strongly hint at the existence of a supplementary polarization mechanism, which saturates rapidly when increasing the dc bias field. The contribution of such a component with quasiswitching properties to the dielectric response is expected to vanish due to its constant saturation value at high fields.

Bearing in mind the proposed random-field nature of the STO18 system,[9,12] the appearance of precursorlike polar clusters is very likely when approaching the phase transition region. They are expected to have an effective polarization P_0 and a volume ϑ. The polarization due to the reorientation of such noninteracting polar regions may be described within a discrete-level Langevin-type approach[29,30]

$$P = P_0 \tanh(P_0 \vartheta E/2k_B T), \tag{8}$$

where the local field is assumed to be close to the external one $E_{\mathrm{loc}} \cong E$. The factor 2 in the denominator is due to the *xy*-type symmetry of the polarization order parameter of

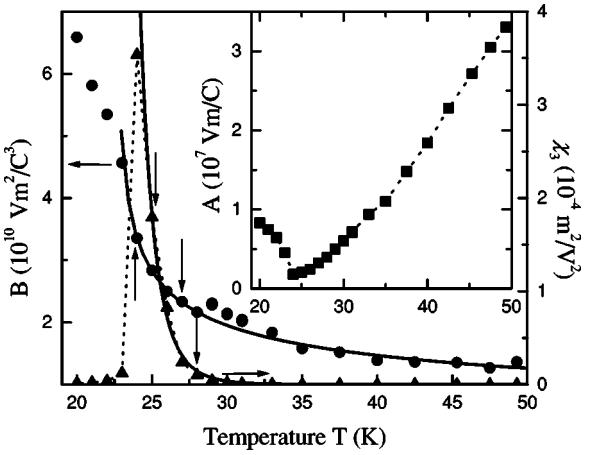

FIG. 4. Temperature dependences of the fitting parameters A (inset), B, and the calculated third order susceptibility χ_3. The solid line represent the best fits within the range shown by vertical arrows with the critical exponents $3\gamma - 2\Delta = -0.33 \pm 0.04$, $T_s = 15.5$ K (fixed), $T_c^Q = 26.9 \pm 0.3$ K, and $B_0 = (1.25 \pm 0.07) \times 10^{10}$ m^5 V/C^3 and $\gamma + 2\Delta = 8.2$ (fixed), $T_s = 15.5$ K (fixed), $T_c^Q = 20.7 \pm 0.5$ K, and $B_0/(\varepsilon_0 A_0^4)$ m^2/V^2, respectively, and extrapolated beyond the fitting range. Dotted lines are to guide the eyes.

STO18 as anticipated by analogy with Ca^{2+}-doped STO16.[4] Equation (8) yields the following expression for the dielectric susceptibility χ_r':

$$\chi_r' = \partial P/\varepsilon_0 \partial E = \chi_{0r}[\cosh(Ex)]^{-2}, \tag{9}$$

where $\chi_{0r} = P_0 x/\varepsilon_0$ and $x = P_0 \vartheta/2k_B T$. As can be seen from the solid line in Fig. 3(b), this additional term together with the previously used Eqs. (3) and (4) definitely improves the quality of the fit. As a consequence, the value of the χ-square function is substantially reduced to $\chi^2 = 249.6$, and the correlation coefficient increases, $R^2 = 0.99998$, while the values of the four fitting parameters are $A = (6.034 \pm 0.002) \times 10^6$ V m/C, $B = (2.25 \pm 0.002) \times 10^{10}$ m^5 V/C^3, $\chi_{0r} = 260 \pm 8$, and $x = (1.90 \pm 0.08) \times 10^{-4}$ m/V. The last two parameters provide the value of effective polarization of the precursor clusters $P_0 = \chi_{0r}\varepsilon_0/x = (1.21 \pm 0.09) \times 10^{-5}$ C/m^2. As seen in Fig. 3(b), the contribution to the total dielectric response (solid line) due to the additional extrinsic polarization mechanism is fairly small (in the order of 1%) and, as expected, it vanishes at very weak fields $E \approx 10$ kV/m [Fig. 3(b), broken line]. Subtracting this contribution it is easy to extract the intrinsic response of the host as represented by the dotted line in the inset of Fig. 3(b). The dynamic heterogeneity thus introduced might be referred to as a multipolarization mechanism model.[31] Here we decided to add a rapidly saturating cluster contribution with superparaelectric switching properties to the background, whose strong field dependence extending to very high fields is excellently described by dielectric nonlinearity.

Using the above procedure it is possible to determine the temperature dependence of the nonlinearity coefficient B which is shown in Fig. 4. As is seen, B increases when approaching the phase transition point from above. It shows a weak relative maximum at 29 K. Since the apex of the sus-

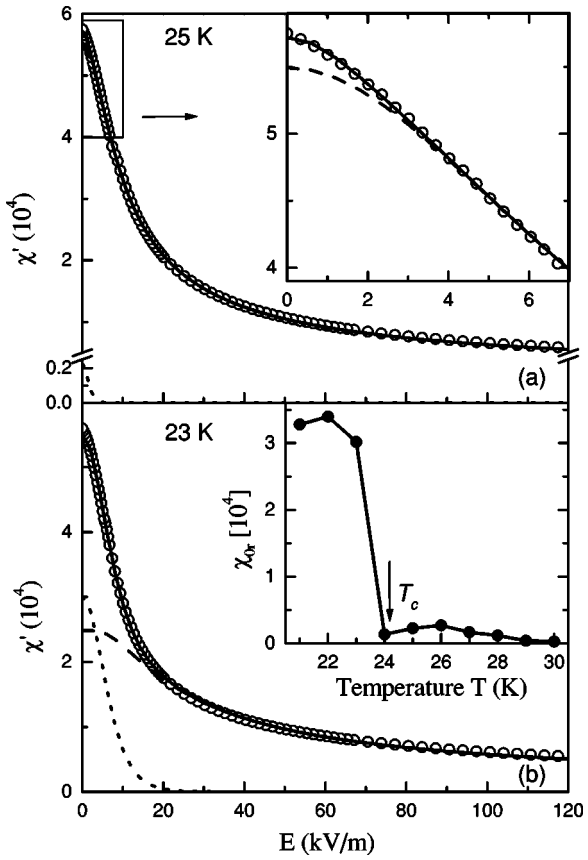

FIG. 5. dc electric field dependences of the electric susceptibility taken at $T=24\pm1$ K, respectively, and their fits according to the two component polarization mechanism (solid lines). The dashed and dotted lines represent the susceptibility related to the intrinsic and extrinsic components of the polarization. The inset in (a) shows details in the low field limit. The inset in (b) shows the temperature dependence of χ'_{0r} (the line is to guide the eyes). The values of the fitting parameters are (a) $A=(2.3\pm0.2)\times10^6$ V m/C, $B=(2.835\pm0.012)\times10^{10}$ m^5 V/C^3, $\chi'_{0r}=(2.3\pm0.2)\times10^3$, $x=(5.5\pm0.7)\times10^{-4}$ m/V and (b) $A=(4.5\pm0.9)\times10^6$ V m/C, $B=(4.56\pm0.05)\times10^{10}$ m^5 V/C^3, $\chi'_{0r}=(3.02\pm0.05)\times10^3$, and $x=(1.400\pm0.015)\times10^{-4}$ m/V.

ceptibility χ' vs E remains localized at $E=0$ below T_c, the above superposition procedure was used for fitting a few isotherms in the ferroelectric state as well.

It is advisable here to demonstrate a fundamental difference in the fitting results of the isotherms above and below T_c. Figure 5 presents two isotherms taken at $T=T_c\pm1$ K and their analysis. While at 25 K the extrinsic reorientation mechanism at $E=0$, χ_{0r}, contributes only 3% to the total response [Fig. 5(a): dotted line], at 23 K it increases significantly up to 46% [Fig. 5(b): dotted line]. The inset to Fig. 5(b) presents the temperature dependence of χ_{0r} with its jumplike increase below T_c. While the intrinsic "bulk" susceptibility decreases by a factor of about 2, as expected at a second order phase transition, the extrinsic "cluster" or "domain" susceptibility increases by a factor of about 20. This is a convincing illustration of the transformation of the STO18 system into a domain state below $T_c=24$ K. We are inclined to call this state a "quantum domain state" since

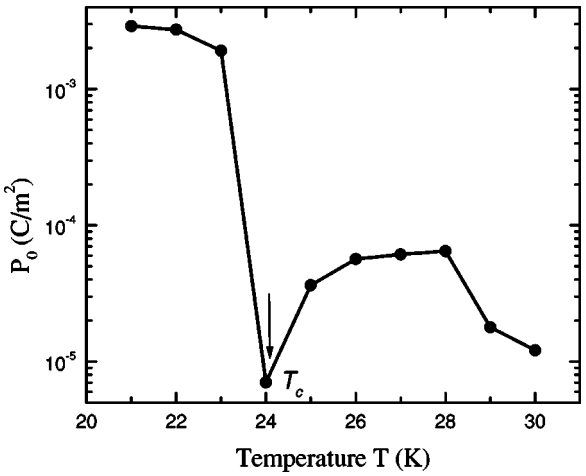

FIG. 6. Temperature dependence of the calculated effective polarization $P_0=\varepsilon_0\chi'_{0r}/x$ of the polar regions. The line is to guide the eyes.

tunneling as a substantial quantum feature is involved in this part of the susceptibility.[8,9] Very probably the fine-grained nature of this state explains the lack of structural changes reported in recent x-ray or neutron-diffraction studies.[5,17] When the system contains a large number of mesoscopic accidentally oriented polar regions, its global symmetry remains unchanged as is wellknown from zero-field cooled cubic relaxor crystals.[32] Symmetry changes on a very small length scale is beyond resolution of a given technique and thus simply cannot be detected. The above picture is supported by very slim hysteresis loops with an extremely small remnant polarization[5] and by the temperature dependence of the effective polarization P_0 of polar regions as presented in Fig. 6. While P_0 shows a sharp drop just above T_c, it increases in a jumplike fashion by two orders of magnitude below T_c. Very probably this kind of behavior does not reflect the real temperature dependence of the spontaneous polarization, since below T_c the dielectric response is completed by considerable domain wall contributions as evidenced by strong dispersion of the dielectric susceptibility that was absent in the paraelectric state. Hence, domain wall contributions are contained and P_0 can neither be considered as the cluster polarization, nor as a measure of the polar order parameter. Similarly, the sharp minima of the fitting parameters χ_{0r} and P_0 are questionable. These parameters were extracted from the near-critical isotherm taken at $T=24$ K, where the system is strongly unstable and small changes in temperature can give rise to large changes in the response. More systematic research addressed to this region is suggested for future experiments.

C. Criticality and scaling properties

Let us come back to the parameters of the intrinsic polarization. When crossing the phase transition point from the paraelectric state the nonlinearity coefficient B jumps up and then increases smoothly again (Fig. 4). The coefficient A, which is proportional to the inverse of susceptibility, shows a pronounced minimum at T_c (see inset in Fig. 4). The third

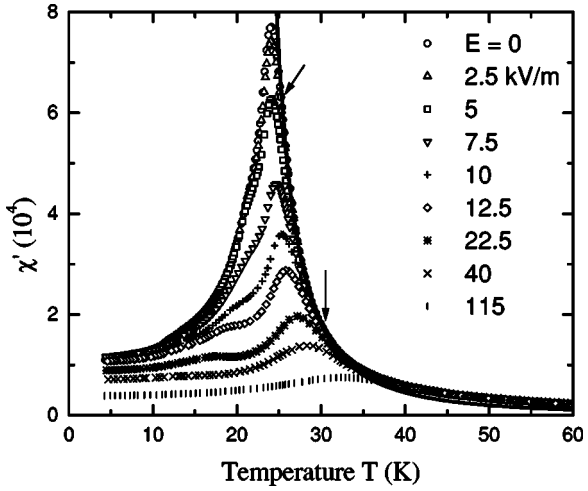

FIG. 7. Temperature dependences of the electric susceptibility at selected dc bias fields. The solid line represents the best fit of the data at $E=0$ within $25.5 \leqslant T \leqslant 31.5$ K with $C=(1.2\pm0.2)\times10^6$, $T_s=15.5$ K (fixed), $T_c^Q=23.8\pm0.2$ K, and $\gamma=1.92\pm0.07$.

order susceptibility $\chi_3=B/(\varepsilon_0 A^4)$ then displays a very sharp maximum at T_c in its temperature dependence (Fig. 4).

In order to characterize the temperature dependence of the coefficient B one should refer to the equation of state written in a more general way,[33]

$$E = A_0|\tau|^{\gamma}P + B_0|\tau|^{3\gamma-2\Delta}P^3, \tag{10}$$

where γ, Δ, A_0, and B_0 are the critical exponent of the susceptibility, the gap exponent, and constants, respectively. Here we propose to replace the classic reduced temperature $\tau=(T-T_c)/T_c$ by its quantum equivalent $\tau^Q=(T^Q-T_c^Q)/T_c^Q$ with $T^Q=T_s \tanh T_s/T$;[34] $T_s=15.5$ K. After this modification the factor in the first term in Eq. (10) is directly related to the generalized quantum Curie-Weiss law (see below), while the second one describes temperature dependence of the nonlinearity coefficient B in the quantum regime. The modified version of the equation of state thus obtained may be referred to as a quantum electric equation of state. When fitting the B data within the interval $24 \leqslant T \leqslant 28$ K one obtains the exponent $3\gamma-2\Delta=-0.33\pm0.04$. Extrapolation beyond the fitting range follows pretty well the rest of data (solid line in Fig. 4). As it is seen, this exponent is determined by the values of γ and Δ which have to be extracted from other sources.

The exponent γ is obtained from the susceptibility measured at vanishing dc bias field (Fig. 7: circles). Fitting these data within the temperature range $25.5 \leqslant T \leqslant 31.5$ K to the generalized quantum Curie-Weiss law[35]

$$\chi' = \frac{C}{(T^Q - T_c^Q)^{\gamma}}, \tag{11}$$

we obtain $\gamma=1.92\pm0.07$ (solid line in Fig. 7), which comes very close to the one predicted for the quantum regime, $\gamma=2$.[36] T_s was fixed after a preliminary fitting procedure in order to reduce the standard deviation of the remaining adjustable parameters. It is worthwhile noticing that a best fit to

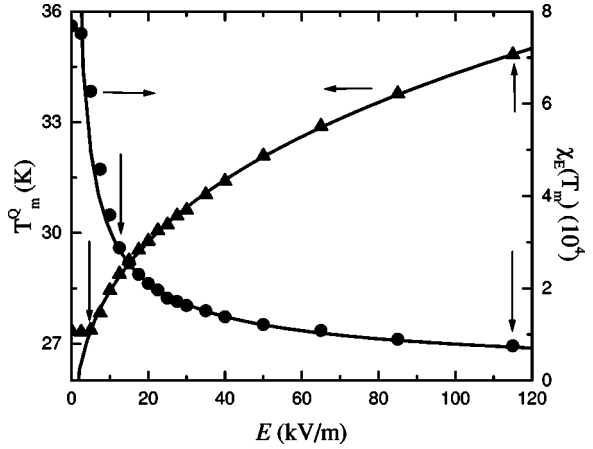

FIG. 8. Dependences of T_m^Q (triangles) and $\chi_E(T_m)$ (circles) on the electric field E. The solid lines represent fits of the data within the range indicated by the vertical arrows to the formulas $T_m^Q=T_c^Q+KE^{1/\Delta}$ and $\chi_E(T_m)=K'E^{-1/a}$, respectively, with $T_c^Q=23.1\pm0.3$ K, $K=2.5\pm0.2$, $\Delta=3.08\pm0.14$, $K'=(1.33\pm0.04)\times10^5$, and $a=1.63\pm0.03$.

Eq. (11) of the data above $T=30$ K yields the mean-field value $\gamma=1$.

When applying a dc field E the maximum value of the susceptibility $\chi_E'(T_m)$ decreases with increasing values of E and its temperature position T_m shifts towards higher temperatures (Fig. 7). According to scaling theory[37] these quantities are scaled by power laws with exponents Δ and $a=\Delta/\gamma$, respectively, as extended to the quantum limit[38]

$$E \propto \left(\frac{T_m^Q(E)}{T_c^Q} - 1\right)^{\Delta} \tag{12}$$

and

$$\chi_E(T_m^Q) \propto E^{-1/a}. \tag{13}$$

These relations provide a possibility for an experimental extraction of the values of these exponents. To this end, first, the T_m data have to be rescaled into quantum temperatures ($T_m^Q \rightarrow T_m$) via the expression given above as shown by triangles in Fig. 8. Within the field $5<E<120$ kV/m we find $T_c^Q=23.1\pm0.3$ K in agreement within errors with the result from Eq. (11) and the gap exponent $\Delta=3.08\pm0.14$. Using the exponent $\gamma=1.92\pm0.07$ (see above), one calculates the exponent $a=1.60\pm0.13$.

On the other hand, the exponent a may directly be obtained when fitting the $\chi_E(T_m)$ vs E data to Eq. (13) (solid line in Fig. 8). We obtain $a=1.63\pm0.03$, which is in a very good agreement with the previous one. Finally, we may calculate, again, the exponent referring to the $B(T)$ data $3\gamma-2\Delta=-0.4\pm0.5$. It is in satisfactory agreement with the previous one (see above). The large error (±0.5) is due to the propagation of the individual standard deviations of particular terms. Obviously, the critical behavior of $B(T)$ is characterized by a divergence. It is clear now that the unusual temperature dependence of the nonlinearity coefficient B, is a consequence of the particular nonclassic values of exponents γ and Δ.

Having in mind the expression for the third order susceptibility $\chi_3 = B/(\varepsilon_0 A^4)$ one easily obtains a respective expression describing its temperature dependence as

$$\chi_3 = \frac{B_0}{\varepsilon_0 A_0^4} |\tau^Q|^{-(\gamma+2\Delta)}. \tag{14}$$

This expression fits satisfactorily to the data presented in Fig. 4 (triangles and respective solid line) with the exponent $\gamma + 2\Delta = 8.2$, which complies well with that obtained from the individual values of γ and Δ, $\gamma + 2\Delta = 8.2 \pm 0.4$.

The exponent a is a key quantity for static nonzero-external-field scaling analysis of the data based on the relation[37,38]

$$\chi'(T,E)/\chi'(T,0) = f\{E[\chi'(T,0)]^a\}, \tag{15}$$

with $a = \delta/(\delta - 1) = \Delta/\gamma$. Here $\chi'(T,E) \equiv \chi'(T)$ is the static dielectric susceptibility at temperature T and external field E, whereas $\chi'(T,0) \equiv \chi_0'(T)$ is the zero-field susceptibility at the same temperature. δ scales the power-law relation of the critical isotherm at $T = T_c$, $E \propto P^\delta$, between the external electric field and the polarization. This equation is very convenient for the scaling analysis of criticality, because it contains only one fitting parameter a and does not require *a priori* knowledge of the critical temperature. In order to check the scaling behavior of the data we constructed the scaling function f according to Eq. (15), $\chi_E'(T)$ vs $E[\chi_0'(T)]^a$ by using different values of a. Best data collapsing onto one master curve is achieved with $a = 1.62$ (Fig. 9) in good agreement with values obtained above. Closer inspections shows that it provides an excellent compromise for almost all data points.

The scaling analysis of the experimental susceptibility data discloses a very good scaling behavior of the STO18 system with consistent effective scaling exponents. Using the well known scaling relations one may calculate further exponents, e.g., $\beta = \Delta - \gamma = 1.2 \pm 0.2$ and $\alpha = 2 - \gamma - 2\beta = -2.1 \pm 0.5$. These values show drastically that STO18 deviates significantly from the classic Landau universality class. They give rise to the unusual temperature dependence of the nonlinearity coefficient B as discussed above. To the best of our knowledge, the result $\beta > 1$ has never been found in any theoretical system. However, the possibility for $\beta > 1$ has already been suggested for the doped system $SrTiO_3$:Ca.[38]

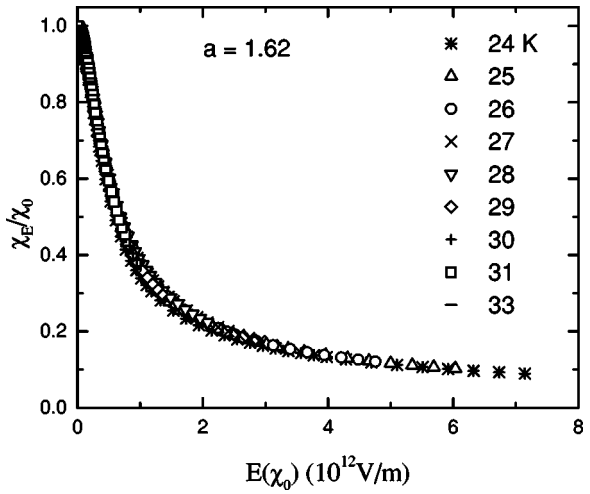

FIG. 9. Dependences of χ_E/χ_0 on $E(\chi_0)^a$. Best data collapsing is achieved with $a = 1.62$. For clarity only every second experimental point is shown.

IV. CONCLUSION

Within the framework of a two component polarization mechanism it has become possible to separate the extrinsic polarization due to reorientation of polar regions from the intrinsic host one. Our exponents thus determined are related to the intrinsic polarization of the system investigated in a structural single domain state. They make the present investigation much more precise than our previous one[19] and enhance its degree of reliability. It should be stressed that, although the relative contribution of the extrinsic polarization to the total response is very low in the paraelectric state, it gives rise to quite sizable changes of the nonlinearity coefficient $B(T)$. However; it increases substantially in the ferroelectric state, which might be classified as a quantum domain state controlled by quenched random fields.

Furthermore it has been shown that the very simple quantum electric equation of state offers a powerful tool for a satisfactory description of the nonlinear dielectric response up to a relatively large field range, even in the case of a very strong field dependence of the dielectric susceptibility. Approximate treatments or truncated series expressions have only limited usefulness.

ACKNOWLEDGMENTS

Financial support by DFG (SPP "Strukturgradienten in Kristallen") is gratefully acknowledged.

*Electronic address: dec@us.edu.pl

[1] V. V. Lemanov, Ferroelectrics **265**, 1 (2002).
[2] K. A. Müller, W. Berlinger, C. H. West, and P. Heller, Phys. Rev. Lett. **32**, 160 (1974).
[3] K. A. Müller and H. Burkard, Phys. Rev. B **19**, 3593 (1979).
[4] J. G. Bednorz and K. A. Müller, Phys. Rev. Lett. **52**, 2289 (1984).
[5] M. Itoh, R. Wang, Y. Inaguma, T. Yamaguchi, Y.-J. Shan, and T. Nakamura, Phys. Rev. Lett. **82**, 3540 (1999).
[6] A. Bussmann-Holder, H. Büttner, and A. R. Bishop, J. Phys.: Condens. Matter **12**, L115 (2000).
[7] O. E. Kvyatkovskii, Solid State Commun. **117**, 455 (2001); Phys. Solid State **43**, 1401 (2001).
[8] Y. Yamada, N. Todoroki, and S. Miyashita, Phys. Rev. B **69**,

024103 (2004).
[9] L. Zhang, W. Kleemann, J. Dec, R. Wang, and M. Itoh, Eur. Phys. J. B **28**, 163 (2002).
[10] L. Zhang, W. Kleemann, R. Wang, and M. Itoh, Appl. Phys. Lett. **81**, 3022 (2002).
[11] R. Blinc (private communication).
[12] R. Wang and M. Itoh, Phys. Rev. B **62**, R731 (2000).
[13] T. Yagi, M. Kasahara, Y. Tsujimi, M. Yamaguchi, H. Hasebe, R. Wang, and M. Itoh, Physica B **316–317**, 596 (2002).
[14] H. Hasebe, Y. Tsujimi, R. Wang, M. Itoh, and T. Yagi, Phys. Rev. B **68**, 014109 (2003).
[15] T. Shigenari, K. Abe, K. Yanashita, T. Takemoto, R. Wang, and M. Itoh, Ferroelectrics **285**, 415 (2003).
[16] E. L. Venturini, G. A. Samara, M. Itoh, and R. Wang, Phys. Rev. B **69**, 184105 (2004).
[17] Y. Uesu, R. Nakai, J.-M. Kiat, C. Ménoret, M. Itoh, and T. Kyomen, J. Phys. Soc. Jpn. **73**, 1139 (2004).
[18] M. D. Glinchuk and V. A. Stephanovich, J. Phys.: Condens. Matter **10**, 11 081 (1998).
[19] W. Kleemann, J. Dec, R. Wang, and M. Itoh, Phys. Rev. B **67**, 092107 (2003).
[20] M. Itoh, T. Yagi, Y. Uesu, W. Kleemann, and R. Blinc, Sci. Technol. Adv. Mater. **5**, 417 (2004).
[21] K. A. Müller, W. Berlinger, M. Capizzi, and H. Gränicher, Solid State Commun. **8**, 549 (1970).
[22] K. Abe, K. Yamashita, Y. Tomita, T. Shigenari, R. Wang, and M. Itoh, Ferroelectrics **272**, 155 (2002).
[23] M. Itoh, T. Azuma, T. Kyomen, K. Iio, K. Yamanaka, and R. Wang, J. Phys. Soc. Jpn. **73**, 1377 (2004).
[24] J. Dec, W. Kleemann, and M. Itoh, Appl. Phys. Lett. **85**, 5328 (2004).
[25] R. Wang and M. Itoh, Phys. Rev. B **64**, 174104 (2001).
[26] K. M. Johnson, J. Appl. Phys. **33**, 2826 (1962).
[27] C. J. F. Böttcher, *Theory of Electric Polarization* (Elsevier, Amsterdam, 1977).
[28] A. K. Jonscher, *Dielectric Relaxation in Solids* (Chelsea Dielectric Press, London, 1983).
[29] J. Dec, W. Kleemann, U. Bianchi, and J. G. Bednorz, Europhys. Lett. **29**, 31 (1995).
[30] U. Bianchi, J. Dec, W. Kleemann, and J. G. Bednorz, Phys. Rev. B **51**, 8737 (1995).
[31] Chen Ang and Zhi Yu, Phys. Rev. B **69**, 174109 (2004).
[32] L. E. Cross, Ferroelectrics **76**, 241 (1987).
[33] E. Stanley, *Phase Transitions and Critical Phenomena* (Clarendon Press, Oxford, 1971), Chap. 11.
[34] E. K. H. Salje, B. Wruck, and H. Thomas, Z. Phys. B: Condens. Matter **82**, 399 (1991).
[35] J. Dec and W. Kleemann, Solid State Commun. **106**, 695 (1998).
[36] T. Schneider, H. Beck, and E. Stoll, Phys. Rev. B **13**, 1123 (1976).
[37] B. Westwański and B. Fugiel, Phys. Rev. B **43**, 3637 (1991).
[38] W. Kleemann, J. Dec, and B. Westwański, Phys. Rev. B **58**, 8985 (1998).